Molecular Microbiology (2013) 87(5), 1074–1087 ■
doi:10.1111/mmi.12150
First published online 6 February 2013

Colocalization and interaction between elongasome and divisome during a preparative cell division phase in *Escherichia coli*

René van der Ploeg,[1] Jolanda Verheul,[1] Norbert O. E. Vischer,[1] Svetlana Alexeeva,[1†] Eelco Hoogendoorn,[2] Marten Postma,[2] Manuel Banzhaf,[3‡] Waldemar Vollmer[3] and Tanneke den Blaauwen[1]*

[1]*Bacterial Cell Biology, Swammerdam Institute for Life Sciences, University of Amsterdam, Science Park 904, 1098 XH Amsterdam, P.O. Box 94232, 1090 GE Amsterdam, the Netherlands.*

[2]*Molecular Cytology, Swammerdam Institute for Life Sciences, University of Amsterdam, Science Park 904, 1098 XH Amsterdam, P.O. Box 94215, 1090 GE Amsterdam, the Netherlands.*

[3]*Institute for Cell and Molecular Biosciences, The Centre for Bacterial Cell Biology, Newcastle University, Richardson Road, Newcastle upon Tyne NE2 4AX, UK.*

Summary

The rod-shaped bacterium *Escherichia coli* grows by insertion of peptidoglycan into the lateral wall during cell elongation and synthesis of new poles during cell division. The monofunctional transpeptidases PBP2 and PBP3 are part of specialized protein complexes called elongasome and divisome, respectively, which catalyse peptidoglycan extension and maturation. Endogenous immunolabelled PBP2 localized in the cylindrical part of the cell as well as transiently at midcell. Using the novel image analysis tool ColiInspector to analyse protein localization as function of the bacterial cell age, we compared PBP2 localization with that of other *E. coli* cell elongation and division proteins including PBP3. Interestingly, the midcell localization of the two transpeptidases overlaps in time during the early period of divisome maturation. Försters Resonance Energy Transfer (FRET) experiments revealed an interaction between PBP2 and PBP3 when both are present at midcell. A decrease in the midcell diameter is visible after 40% of the division cycle indicating that the onset of new cell pole synthesis starts much earlier than previously identified by visual inspection. The data support a new model of the division cycle in which the elongasome and divisome interact to prepare for cell division.

Accepted 2 January, 2013. *For correspondence. E-mail t.denblaauwen@uva.nl; Tel. (+31) 205255196; Fax (+31) 205257934. Present addresses: †Top Institute Food and Nutrition (TIFN), Wageningen, the Netherlands; Laboratory of Food Microbiology, Wageningen University and Research Centre, Wageningen, the Netherlands; ‡Harvard Medical School, Immune Disease Institute, 3 Blackfan Circle, Boston, 17, MA 02115, USA.

Introduction

Cells of the rod-shaped *Escherichia coli* grow by length growth, i.e. cell elongation, and cell constriction, i.e. new cell pole synthesis. During cell elongation peptidoglycan precursor (lipid II) is dispersedly incorporated into the cylindrical part of the cell wall whereas the new cell poles are synthesized from completely new peptidoglycan (de Pedro *et al.*, 1997). Peptidoglycan is a network of glycan chains cross-linked by peptides and its well-regulated enlargement during growth ensures the osmotic stability and distinct morphology of the cell (Typas *et al.*, 2011). Penicillin-binding proteins (PBPs) catalyse peptidoglycan growth and maturation. The *E. coli* class A (bi-functional) PBPs PBP1A, PBP1B and PBP1C have glycosyltransferase and transpeptidase activities. The class B PBPs are monofunctional transpeptidase proteins that cross-link peptidoglycan subunits (Sauvage *et al.*, 2008). Two of these, PBP2 and PBP3, are present in *E. coli* and they have different cellular functions (Spratt, 1975): inactivation or depletion of PBP2 leads to spherical cells due to inhibition of cell elongation, whereas inactivation or depletion of PBP3 results in filamentous cells due to a block in new cell poles synthesis.

Lateral cell wall synthesis is accomplished by a protein complex called elongasome (den Blaauwen *et al.*, 2008) that is assumed to be recruited by the actin-like MreB, which is essential for length growth. MreB can form filaments (Jones *et al.*, 2001) and is attached to the inner side of the cytoplasmic membrane with its N-terminal amphiphatic helix (Salje *et al.*, 2011). Recent evidence supports dynamic segments of MreB driven by ongoing peptidoglycan synthesis in *Bacillus subtilis* (Dominguez-Escobar *et al.*, 2011; Garner *et al.*, 2011) and *E. coli* (van Teeffelen *et al.*, 2011; Swulius and Jensen, 2012; Wang *et al.*, 2012).

MreB is associated with other essential cell elongation proteins of unknown functions including the integral membrane protein MreD, the bitopic membrane proteins MreC and RodZ, which assists in the assemblage of MreB (Kruse *et al*., 2005; Bendezu *et al*., 2009). Based on bacterial two-hybrid assays, immunoprecipitation, affinity chromatography and localization studies, the elongasome contains other proteins that include the lipid II peptidoglycan precursor synthesizing Mur enzymes and MraY (Mohammadi *et al*., 2007; White *et al*., 2010), the hypothetical lipid II translocase RodA (Mohammadi *et al*., 2011) up to the peptidoglycan synthesizing Class A and B PBPs (den Blaauwen *et al*., 2008; Sauvage *et al*., 2008; Vollmer and Bertsche, 2008; Banzhaf *et al*., 2012).

The construction of new cell poles requires PBP3 at midcell together with about 20 essential and non-essential cell division proteins. Correct positioning of these proteins for normal cell pole synthesis requires a period of preparation, which is part of the cell division process (Aarsman *et al*., 2005; Goehring and Beckwith, 2005). Cell division is therefore initiated well in advance of the cell pole synthesis and starts with the polymerization of FtsZ in a ring-like structure at midcell (Bi and Lutkenhaus, 1991; Fu *et al*., 2010). FtsA and ZipA anchor FtsZ to the cytoplasmic membrane (Wang *et al*., 1997; Hale and de Boer, 2002). Subsequently, the Z-ring recruits a set of later localizing proteins that synthesize the new cell poles. The recruitment of the majority of the proteins involved in cell division, or divisome maturation, takes about 20% of the division cycle time after the localization of the Z-ring (Aarsman *et al*., 2005; Goehring and Beckwith, 2005). When the maturation of the divisome is prevented but not the assemblage of the Z-ring, still a band of completely new peptidoglycan (preseptal peptidolgycan) is synthesized at midcell (Varma *et al*., 2007; Varma and Young, 2009; Olrichs *et al*., 2011; Potluri *et al*., 2012), despite the fact that the Z-ring and the early localizing cell division proteins are not known to synthesize peptidoglycan.

GFP–PBP2 localizes transiently at midcell and its activity is required to maintain the correct diameter of the new cell poles (den Blaauwen *et al*., 2003). Also the essential cell elongation proteins MreB, MreC and MreD localize transiently at midcell when fused to fluorescent proteins (Vats *et al*., 2009). Therefore, the elongasome seemed to be the most likely candidate for the synthesis of this preseptal peptidoglycan band in the absence of a functional or mature divisome. Using antibodies directed against the endogenous PBP2, we now confirm the localization pattern of GFP–PBP2 (den Blaauwen *et al*., 2003) and extend these studies in much more detail. In addition, the relation between the localization of the elongasome proteins MurG, MreB and PBP2, the early localizing FtsZ and the late localizing proteins PBP3 and FtsN are explored in detail in thousands of cells as function of the progression of the division cycle. Although the divisome maturation still takes about 20% of the division cycle, the FtsZ proteins positioning at midcell occurs at an earlier age than was found in our previous studies based on visual inspection of the localization patterns (Aarsman *et al*., 2005). Remarkably, we observed a clear overlap between the midcell localization of PBP2 and PBP3 during an early phase in divisome maturation. This prompted us to investigate whether these proteins interact. By using an *in vivo* Försters Resonance Energy Transfer (FRET) technique (Alexeeva *et al*., 2010) we show that PBP2 homodimerizes and that the colocalizing PBP2 and PBP3 proteins interact only when they are both present at midcell. The time window of this colocalization coincides with a preparative phase in division that could match preseptal peptidoglycan synthesis. We propose that the transient positioning of the elongasome and divisome proteins at midcell assist in the fine-tuning of the correct positioning of the synthesis of the new cell poles. In addition, peptidoglycan synthesis in the lateral wall decreases when elongasome complexes move to midcell (Wientjes and Nanninga, 1989). As cell pole synthesis contributes considerably to the length growth of the bacterium, perhaps the recruitment of elongasomes to the Z-ring keeps the overall length growth exponential while the new cell poles are synthesized.

Results

PBP2 and PBP3 localization overlaps at midcell during early divisome maturation

PBP2 is essential for length growth and consequently GFP–PBP2 was observed to localize in the cylindrical part of the cell (den Blaauwen *et al*., 2003). Surprisingly, GFP–PBP2 was also found to accumulate transiently at midcell. Inhibition of PBP2 in wild-type cells caused the new cell poles to increase in width before any other part of the cells changed in shape (den Blaauwen *et al*., 2003). This suggested that PBP2 localization to midcell is important to control the diameter of the new cell poles. At that time GFP–PBP2 was expressed from a plasmid. Here PBP2-specific antibodies were used to obtain a presentation of the localization of the endogenous PBP2 protein (Figs 1A and B and 2). The specificity of the antiserum is shown in supplementary Fig. S1.

To be able to interpret the localization of PBP2 in the framework of divisome maturation time, we analysed the topography of immunolabelled well-known early and late localizing cell division proteins. In previous work the localization of the divisome proteins FtsZ, FtsQ, FtsW, PBP3 and FtsN were studied by visually determining the position of an immunolabelled or fluorescent fusion protein (Aarsman *et al*., 2005). For each protein about 500 cells were analysed for the presence of a fluorescent band at

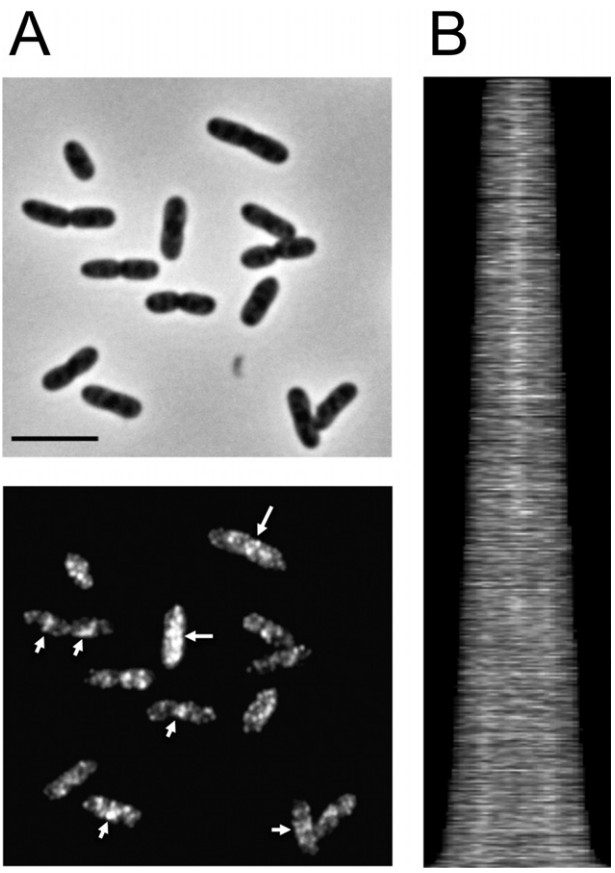

Fig. 1. Immunolocalization of PBP2 in LMC500 wild-type *E. coli* cells grown in TY at 28°C.
A. Examples of labelled cells. At the top a phase-contrast image and at the bottom the corresponding fluorescence image are shown. Arrows point at division sites with PBP2 localization. The bar equals 5 μm.
B. The map of fluorescence profiles of 4389 cells sorted according to their length. The total integrated fluorescence of each cell is plotted as function of its cell length (*x*-axes) and all cells are plotted with increasing cell length from top to bottom (*y*-axes).

midcell. Labelling steady state grown cells enables calculation of the cell age at which a protein localizes at midcell (Aarsman *et al.*, 2005). These studies revealed localization of FtsZ after 40% of the division cycle and for FtsQ, FtsW, PBP3 and FtsN midcell presence was found to be at a later stage (60% of the division cycle). The process was described as divisome maturation in two steps (Aarsman *et al.*, 2005). We have now developed an automated cell counting and analysing macro called Coli-Inspector that is used in combination with the image analysis program ObjectJ to obtain more objective quantitative data. This program allows the analysis of thousands of cells at a speed of 400 cells per min and greatly improves the reliability by which the timing and topography of proteins in the cells can be determined.

Wild-type LMC500 cells were grown to steady state in minimal glucose medium at 28°C, fixed and immunolabelled with antibodies directed against MurG, MreB, PBP2, FtsZ, PBP3 and FtsN. Between 2000 and 5000 cells were analysed by Coli-Inspector/ObjectJ with respect to cell shape and fluorescence distribution for each protein. Besides quantitative data, the Coli-Inspector macro also returns a qualitative but very direct visualization of the analysis in the form of a sorted map of profiles showing either the diameters derived from the phase-contrast images or the fluorescence derived from the fluorescence images of all the individual cells as function of cell length (Fig. 2). In these maps, the appearance of a constriction (map of diameter profiles) or the timing of the localization at midcell of proteins (map of fluorescence profiles) are immediately visible. In addition, cells were stained with the general membrane stain Bodipy-12 to be able to compare complete membrane fluorescence in contrast to the specific localization of the membrane embedded proteins.

Midcell localization of proteins was quantified in the following way. The deviation of cellular fluorescence at midcell (FCplus) was calculated. The mean FCplus of age classes of cells in the population together with their corresponding 95% confidentiality interval were plotted against the progression in division cycle time shown as percentage of cell age (see supplementary Fig. S2 for graphs of the raw data). The mean FCplus was normalized between the minimal and maximal values of the fluorescence to enable a concentration independent comparison between the various proteins (Fig. 3).

The addition of fixative to the shaking culture flask caused an increase in the osmolarity of the medium. To verify that this did not affect the localization pattern of PBP2 (Hocking *et al.*, 2012) cells expressing GFP–PBP2 before (living) and after addition of the fixative were compared. No difference in localization pattern of GFP–PBP2 in the living or fixed cells was observed (results not shown). Detected by antibodies, the native PBP2 localized in the cylindrical part of the cells and transiently at midcell, confirming the earlier fluorescence localization of GFP–PBP2 (Fig. 1) (den Blaauwen *et al.*, 2003). Cells grown in TY at 28°C with a mass doubling time of 40 min spend most of their division cycle time dividing. Therefore, not surprisingly, the map of fluorescence profiles from these cells shows midcell localization for PBP2 in the shortest cells, and PBP2 has already moved to the midcell of the future daughter cells in the longer cells (Fig. 1B). In cells grown in minimal medium with a generation time of 85 min the PBP2 signal increased simultaneously with the appearance of FtsZ at midcell after 20% of the division cycle (Fig. 3A and Table 1). It reached a maximum at 30% and then slowly decreased to a constant level at 60% of the division cycle when the constriction process speeds up (Fig. 3A). Thus, PBP2 is enhanced at midcell for a period of about 40% of the *E. coli* division cycle (Fig. 3A).

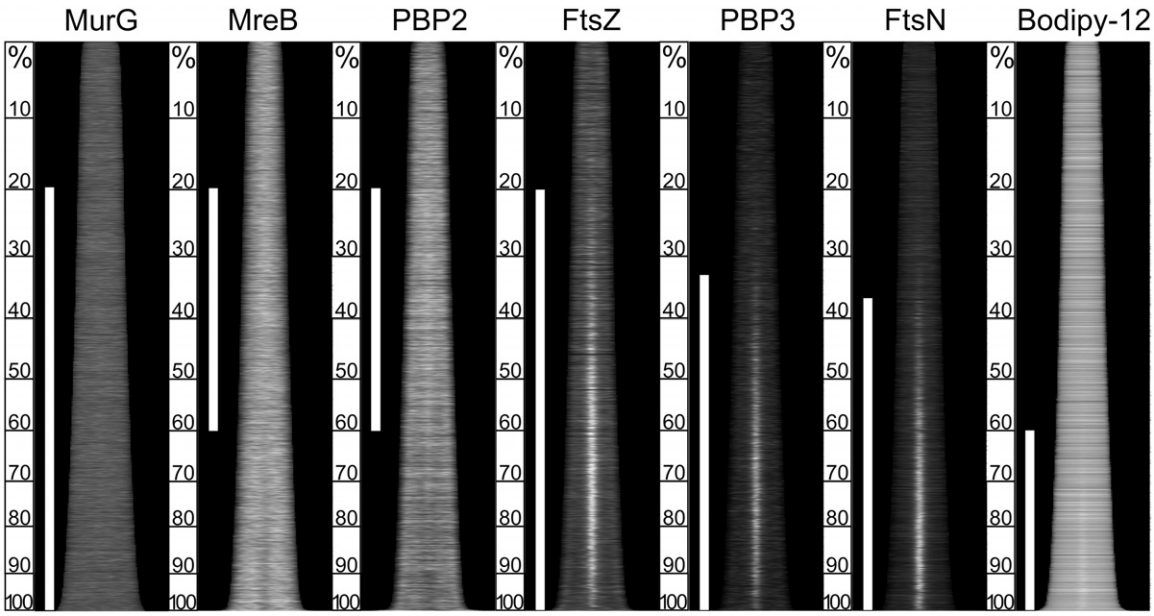

Fig. 2. Map of fluorescence profiles of LMC500 wild-type cells grown to steady state in GB1 medium at 28°C. The membrane is visualized with the general membrane stain Bodipy-12. MurG, MreB, PBP2, FtsZ, PBP3 and FtsN were immunolocalized. On the left of each profile the division cycle time in percentages is given. The white bar indicates in the case of Bodipy-12 the region of double membranes at midcell. For MurG, MreB, PBP2, FtsZ, PBP3 and FtsN the white bars present midcell localization judged by visual inspection. Each map was made from 2000 to 4000 cells. The integral fluorescence of each cell is plotted as function of cell length (*x*-axes) and all cells are plotted with increasing age (*y*-axes).

The general membrane strain Bodipy-12 (Fig. 3A) illustrates the FCplus signal for unspecific membrane binding. It increases continuously because in newborn cells on average the amount of membrane is higher due to the presence of the cell poles than in the 0.8 μm midcell cylindrical part that is used to calculate FCplus. When the cells grow and start to constrict new membrane becomes available for the Bodipy-12 staining, which causes the FCplus to continue to increase. Due to the fluorescence contribution of the old cell poles the Bodipy-12 stain is not a good indication for the beginning of a constriction. In sharp contrast to the membrane staining by Bodipy-12 the cell poles do not contribute to the signal of PBP2, illustrating that PBP2 is absent in the old poles.

The maps of fluorescence profiles show that PBP3 and FtsN localize later than FtsZ (Fig. 2). Inspection of the extra fluorescence at the cell centre of these proteins revealed that the FCplus signal of FtsZ starts to increase above the Bodipy-12 level at 20% whereas PBP3 and FtsN increase above the Bodipy-12 level after about 38% and 48% of the division cycle respectively (Fig. 3B and Table 1). This is earlier than found upon visual inspection (Aarsman *et al*., 2005). The fluorescence intensity of FtsZ at midcell starts to level just after 50%, which is 20% earlier than PBP3 that reached this point at 70%. FtsN localization lags behind and reaches its maximum midcell fluorescence very late at about 90% of the division cycle.

The time window of PBP2 midcell localization overlaps with the accumulative phase of FtsZ, PBP3 and FtsN localization at midcell. This suggests that the elongasome and divisome transiently colocalize and are possibly simultaneously active at midcell. Because MreB is part of the elongasome and FP-MreB was reported to be at midcell during a short period (Vats *et al*., 2009), we also asked whether the endogenous MreB localized during this period at midcell. In the map of fluorescence profiles of these cells no obvious midcell localization of MreB could be seen (Fig. 2). Interestingly, the FCplus plot did show extra fluorescence at midcell that followed the increase and decrease of PBP2 (Fig. 3D and Table 1). MreB is present in 100-fold excess (Karczmarek *et al*., 2007) to PBP2 (Dougherty *et al*., 1996). As the membrane is overall more covered by MreB than by PBP2, it is possible that a potential small increase in midcell localization of MreB is obscured by the other MreB molecules and so less noticeable than in PBP2 maps of fluorescence profiles (Fig. 2). In the map of fluorescence profiles of cells that are grown in TY the extra MreB fluorescence at the beginning of the division cycle is clearly visible and overlaps with the period at which PBP2 localizes at midcell in cells grown in TY (Fig. S3E). These localization data indicate that the elongasome and the divisome are simultaneously but transiently present at midcell. If this transient localization would also be accompanied by locally new peptidoglycan synthesis one would expect MurG to be

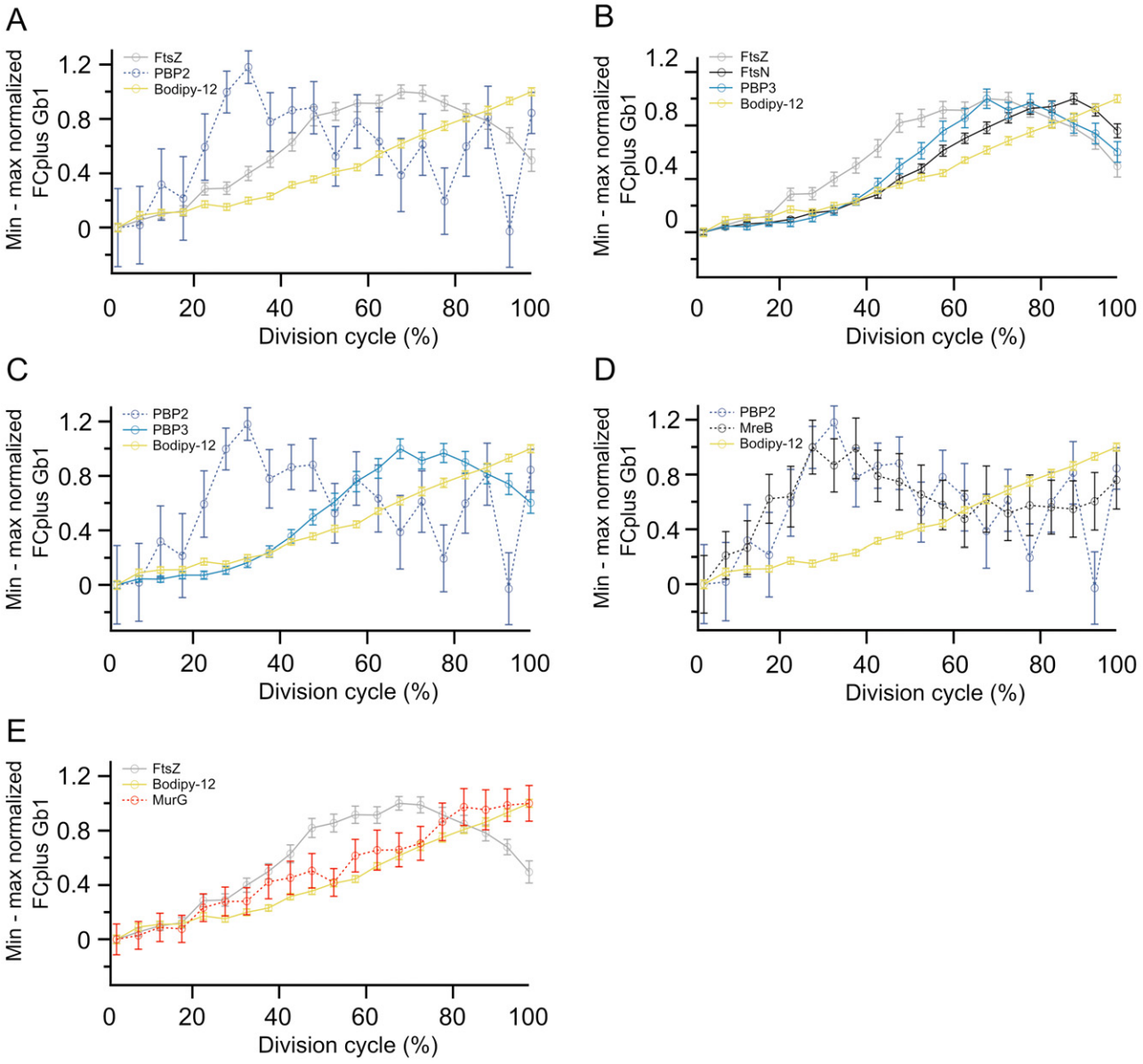

Fig. 3. The quantified signal (FCplus) of midcell fluorescence of immunolabelled or Bodipy 12-stained wild-type LMC500 cells. Cells were grown to steady state in GB1 medium at 28°C. The total number of cells is divided in age classes of 5%, the error bars indicate the 95% confidence interval. The difference in fluorescence between the 0.8 μm cell centre and the remainder of the cell (FCplus) is plotted as a function of the division cycle time in percentages. For concentration independent comparison the data are normalized between their minimum and maximum values. In all graphs the Bodipy-12 FCplus is shown and in addition.
A. PBP2 and FtsZ.
B. FtsZ and the later localizing proteins PBP3 and FtsN.
C. PBP2 and PBP3.
D. MreB and PBP2.
E. MurG and FtsZ.
The original data are presented in the supporting information (Fig. S2).

present as well. Because MurG is the enzyme responsible for the last step in lipid II synthesis and it localizes in the cyclindrical part in an MreCD-dependent fashion as well as at midcell during division (Mohammadi *et al.*, 2007; White *et al.*, 2010). Indeed, we observed a slightly higher level of MurG compared with the Bodipy-12 staining simultaneously with the appearance of FtsZ and PBP2 at midcell (Fig. 3 and Table 1). In conclusion, PBP2, MreB and MurG localize at midcell simultaneously with the positioning of FtsZ proteins.

To address whether this shared localization timing also overlaps with cell pole synthesis we derived the relative

Table 1. The maximal midcell fraction of immunolabelled proteins.

Immunolabelled protein	Maximum value (%)[a]	Initiation (%)[b]	Moment (%)[c]
FtsZ	31.4 ± 1.4	20	72.5
PBP3	33.0 ± 2.1	38	67.5
FtsN	42.0 ± 2.2	48	87.5
MreB	8.3 ± 1.1	18	27.5
PBP2	4.4 ± 1.4	22	27.5
MurG	n.a.[d]	20	n.a.[d]

a. Maximum value is the value at the time point corresponding to the moment. The value is the mean midcell fraction, which is the mean of 100 * FCplus/Fluortotal per cell for all cells at a particular cell division cycle time point.
b. Initiation is the time point in the division cycle where the FCplus from that point onwards is higher than that of Bodipy-12. For MreB and PBP2 it is the moment at which FCplus starts to increase rapidly in comparison with the previous time points.
c. Moment is the time point in the cell division cycle that the midcell fraction is highest.
d. After 20% of the division cycle MurG runs continuously above the Bodipy-12 signal without a maximum.

midcell diameter from the phase-contrast images of the cells (Fig. 4). To obtain an accurate timing of the constriction period, LMC500 cells were grown to steady state in GB1 medium at 28°C and fixed before imaging to maximize the preservation of the cellular morphology. The relative midcell diameter was calculated by taking the smallest diameter at midcell and normalized it to the cylindrical diameter, which is the average cell diameter excluding the poles and constriction site, to remove small diameter variation in the cell population. The relative midcell diameter was plotted as function of the division cycle time (Fig. 4). Interestingly, the diameter of the cylindrical part appeared to be constant during the division cycle. The relative minimal midcell diameter started to deviate from a constant value after 40% of the division cycle and a clear decrease can be seen from 60% of the division cycle onward. The diameter does not decrease to zero because of the limitation of the resolution of the phase-contrast images. However, when the data points are fitted with a simple exponential decay, the diameter is reduced to zero at about 100% of the division cycle. The same constriction behaviour was observed in the immunolabelled cells and in the Bodipy-12-stained cells (not shown). Indicating that the early constriction onset at 40% is not an artefact or single incident and fits with earlier published data where it was found to start at about 50% (Reshes *et al.,* 2008). The constriction phase after 60% of the division cycle corresponds most likely to the synthesis of the new cell poles as it coincides with the localization of a mature divisome (Fig. 3B). Interestingly, during this constriction phase the PBP2 concentration at midcell decreased below the Bodipy-12 signal. This suggests that PBP2 is not present in the new poles that are synthesized (Fig. 3). Therefore, the simultaneous but transient increase of both the elongasome and the divisome proteins at midcell correlated with the decrease in diameter in the period between 40% and 60% of the division cycle, which could be a preparative phase in envelope constriction.

PBP2 interacts with divisome proteins

The resolution of a widefield or confocal microscope is inadequate to determine whether PBP2 and PBP3 colocalize or are just near each other. Therefore, we investigated whether we could measure an interaction by FRET

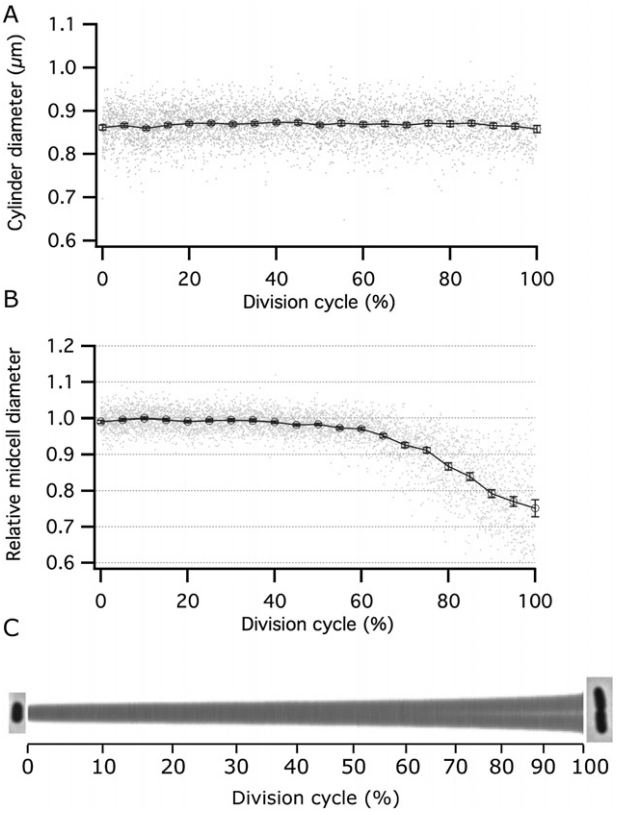

Fig. 4. The diameters of LMC500 wild-type cells grown to steady state in GB1 medium at 28°C with a mass doubling time of 85 min.
A. Graph of the average diameter along the cylindrical part of cells from 20–30% and 70–80% of the cell length (excluding the old cell poles and the newly emerging poles) plotted against the division cycle (cell age). The diameter of the cylindrical part shows no visible change during the cells lifetime.
B. The relative midcell diameter (i.e. the minimal diameter at the centre of the cell divided by the diameter of the cylindrical part of the cell) plotted against division cycle. The dots in the graphs are the values for the individual cells and the line is drawn between the markers that are the mean values with their 95% confidentially interval.
C. The map gives a visual impression of lengths and diameters of all 5000 cells, sorted on length. Each cell is shown as a line representing the cell length, the darkness of the line represents the diameter of the cell. After 60% a band with an increasing width and decreasing intensity can be observed in the middle of the cells, it shows the progress of cell constriction.

between the elongasome and divisome proteins. PBP2 was chosen as representative of the elongasome and FtsZ, ZapA, PBP3, FtsW, FtsQ and FtsN were chosen for divisomal proteins. These proteins were expressed as fusions with fluorescent mKO and mCherry to monitor their localization as well as potential interactions. The mKO and mCherry pair has a relative high Förster radius of 6.37 nm and their excitation produces negligible autofluorescence, which makes them very suitable for the measurement of FRET in bacteria (Alexeeva *et al*., 2010). The constructed N-terminal fusion proteins behaved like wild-type endogenous proteins with respect to their localization (Alexeeva *et al*., 2010) and complemented temperature-sensitive versions of the protein at the non-permissive temperature (den Blaauwen *et al*., 2003; Pastoret *et al*., 2004; Piette *et al*., 2004; Aarsman *et al*., 2005). The fusion proteins were expressed in the wild-type LMC500 strain that was grown to steady state in GB1 at 28°C. Protein expression was induced with 10–15 μM IPTG from low-copy-number plasmids for about 6 h while keeping the optical density at 450 nm below 0.2. The cells were fixed and washed in PBS. The FRET efficiency was calculated from the mCherry and mKO spectra of each sample as previously described (Alexeeva *et al*., 2010). FRET only occurs when the fluorophores of mCherry and mKO are sufficiently close together within a distance of less than 10 nm. With this technique we have detected previously multiple division protein interactions including homo-dimeric complexes of PBP3 (Alexeeva *et al*., 2010; Fraipont *et al*., 2011).

A FRET acceptor efficiency (E_{fA}) of 1.2% found for membrane-bound non-interacting pairs represents the percentage of bystander FRET in the membrane (Alexeeva *et al*., 2010). Using this threshold we have identified interactions of PBP2 with itself and between PBP2 and FtsQ, FtsW, PBP3 and FtsN, but not with FtsZ or ZapA (Fig. S4). A tandem fusion of mKO and mCherry was included as positive control and the combination of PBP1A and PBP3, that do not interact, was included as a negative control in every experiment. Notably, the PBP1A fusion protein is able complement and localize in the EJ801 strain that lacks the *mrcB* and encodes a temperature-sensitive *mrcA* gene. From these results it can be concluded that PBP2 and PBP3 colocalize and possibly interact.

PBP2 and PBP3 interact at the division site

Because the FRET is measured in the entire cell population it does not provide spatial information. To establish if the colocalization of PBP2 and PBP3 occurs only at the division site and not in the cylindrical part of the cells, we have used two mutants of PBP3 that fail to localize at midcell during divisome maturation (Weiss *et al*., 1999; Wissel *et al*., 2005); one with the amino acid change F24A and the other with the transmembrane spanning segment (TSS) replaced by that of MalF (IFI). Both proteins have an unaltered catalytic domain but are not able to localize at midcell in the presence of the endogenous PBP3 protein. Their expression level is similar to that of the wild-type protein and they are stable without degradation (Weiss *et al*., 1999; Wissel *et al*., 2005). The F24A but not the IFI mutant is able to complement some of the temperature-sensitive PBP3 mutant strains (Weiss *et al*., 1999; Wissel *et al*., 2005).

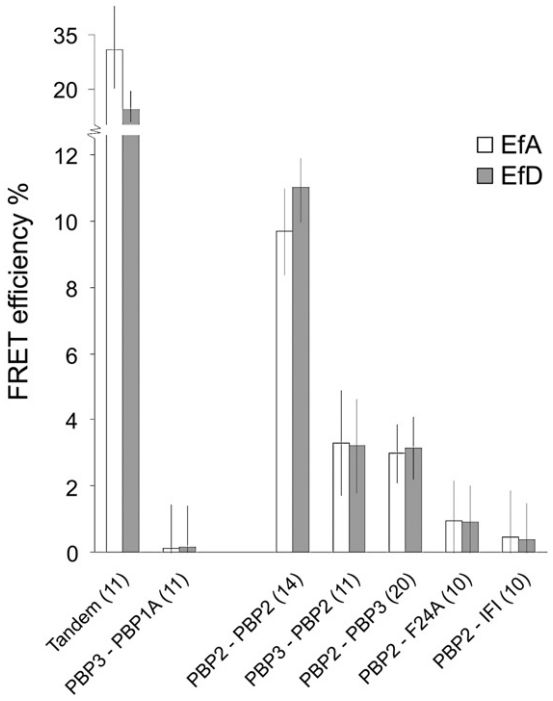

Fig. 5. Interaction between PBP2 with either PBP3 or PBP3 mutant proteins. The expression of donor and acceptor fusion proteins was induced in exponential growing culture at 28°C for 6 h by the addition of 10–15 μM IPTG keeping the OD_{450} below 0.2. The FRET efficiency was calculated from donor and acceptor fluorescence spectra of the cells (Alexeeva *et al*., 2010). In the graph on the left the FRET efficiency of the mCherry–mKO tandem positive control, next the negative control PBP3 with PBP1A and continuing the FRET efficiency of PBP2 with PBP3 and the PBP3 mutants, F24A and IFI. The number of independent repetitions is indicated after the sample name between parentheses. The error bars indicate the 95% confidence interval for each sample. The energy transfer is calculated to yield *Ef*A and *Ef*D representing the apparent FRET efficiencies of the acceptor and donor respectively.

The FRET experiments with PBP2 and the two PBP3 mutant versions gave signals barely above that of the negative control of PBP3 and PBP1A and significantly below the signal for the interaction between PBP2 and PBP3. Indicating that the mutants did not interact with PBP2 (Fig. 5). As both mutants did not localize at midcell, it can be concluded that PBP2 only interacts with PBP3 when it is part of the division machinery at midcell.

PBP2 and PBP3 localization dependence

Are PBP2 and PBP3 mutually dependent on each other for localization at midcell? The LMC582 strain expresses a PBP2(P481S) version from the chromosome that is unstable at 42°C. After two mass doublings at the restrictive temperature PBP2 is not detectable on immunoblot and in immunolabelled cells a diffuse localization is observed (Figs S1 and S5). The instability of PBP2(P481S) causes spherical cell shape already at the permissive temperature. At both, the permissive and restricted temperatures, MreB, FtsZ and PBP3 localize in these cells like in the wild-type situation confirming that the divisome does not need PBP2 for localization (Vinella *et al*., 1993). LMC510 expresses a labile PBP3(G191D, D266N) version (Fig. S1) that causes already at the permissive temperature a delay in division and that fails to support cell division at 42°C. PBP2 localizes very faintly at ¼ and ¾ position in the youngest cells at the restricted temperature whereas PBP3 localization is completely lost (not shown). The localization of PBP2 at division sites is intrinsically weak, therefore the localization in LMC512 cells expressing FtsA(ts) and in JLB17 expressing the FtsW(G113D) temperature-sensitive version (Pastoret *et al*., 2004) were analysed. FtsW forms a complex with PBP3 and both are recruited to midcell (Pastoret *et al*., 2004; Fraipont *et al*., 2011). In the FtsA(ts) strain PBP2, PBP3 and FtsN localized weakly at ¼ and ¾ position in young cells, with the localization of PBP2 barely visible, in contrast to the pronounced localization of FtsZ at these positions (Fig. S6). PBP2 and PBP3 failed to localize in the FtsW(ts) strain at the restrictive temperature (data not shown). Hence, PBP3 or other late localizing proteins are required for the localization of PBP2, which becomes either very faint or absent when PBP3 does not localize at midcell. Clearly, divisome maturation is important for PBP2 midcell localization but the exact factor triggering PBP2 to midcell is as yet unidentified.

Inactivation of PBP2 or PBP3 stimulates midcell localization

Some morphogenetic proteins such as PBP1B, LpoB and PBP5 have been found to be attracted to the division site by ongoing peptidoglycan synthesis (Bertsche *et al*., 2006; Potluri *et al*., 2010; Typas *et al*., 2010) at that site. Therefore, we investigated whether inhibition of PBP2 by mecillinam and of PBP3 by aztreonam would affect their localization. The inhibited PBP2 and PBP3 localized profoundly at all possible division sites (Fig. S7). In case of the spherical mecillinam-treated cells, both proteins localized at the cell division plane with PBP2 also present in the very short cylindrical part of the cells. In addition, the localization of MreB was not disturbed in these cells (Karczmarek *et al*., 2007). In the presence of aztreonam, the division machinery including PBP3 is not able to synthesize new cell poles and stays in a frozen mature form for at least one generation at midcell and to a much lesser extend new localizations occur at ¼ and ¾ of the cell length. PBP2 mimicked this localization pattern in that it was present at midcell less pronounced and at future division sites somewhat more pronounced than PBP3. This is in correspondence with earlier observations that the number of cell with GFP–PBP2 midcell localization decreases when aztreonam is added to the growth medium (den Blaauwen *et al*., 2003). At that time and without the now available Coli-Inspector tool, the weak signals of diffused localization of PBP2 or PBP3 at future division sites were not detectable. This difference in intensity at the various positions is consistent with the early divisome localization of PBP2 and the later localization of PBP3 in wild-type cells (Fig. 2). In addition, PBP2 and PBP3 still interacted in the inhibited cell cultures when assayed by FRET (results not shown). In conclusion, the inhibition of either transpeptidase activity leads to a prolonged localization of PBP2 and PBP3 at division sites, retarding the midcell turnover of these proteins.

Discussion

Cell division proteins orchestrate the synthesis of new cell poles. They move to midcell in a particular order building a complicated but delicate divisome complex in two steps. These steps are called ‘early’ and ‘late’ based on a delay in the localization of a subset of proteins that are required for the actual synthesis of the new cell poles (Aarsman *et al*., 2005). During the early stage of cell division the Z-ring is formed. In the absence of further maturation of the division machinery a small band of completely new peptidoglycan is synthesized at the position of the Z-ring (Varma *et al*., 2007; Varma and Young, 2009; Olrichs *et al*., 2011; Potluri *et al*., 2012) that has been termed preseptal peptidoglycan. In *Caulobacter crescentus* the localization of FtsZ initiates a period of completely new local peptidoglycan synthesis before septation occurs (Aaron *et al*., 2007). This requires the recruitment of MurG that synthesizes the last step in lipid II biosynthesis. As the early localizing proteins that form the Z-ring do not have peptidoglycan synthesizing activities other proteins such as PBPs must be responsible for this preseptal peptidoglycan synthesis. Previously, we showed that GFP–PBP2 is not an integral part of the divisome complex, but is only transiently located at midcell and that its presence is important to maintain the correct diameter of the new cell poles (den Blaauwen *et al*., 2003). In the present study we quantitatively compared the cellular distribution of the elongasome proteins MurG, MreB and PBP2 and the divisome proteins, FtsZ, PBP3 and FtsN as a function of cell age of thousands of cells using immu-

nolocalization of endogenous proteins. We show that the elongasome proteins MreB and PBP2 arrive at midcell simultaneously with FtsZ. Interestingly, both MreB and PBP2 stay there temporarily from 20% to about 60% of the division cycle. After 60% of the division cycle constriction speeds up and the FCplus signal of MreB and PBP2 decreases and remains below the Bodipy-12 signal. This suggests that they are not present in the new poles that are synthesized. The period of midcell localization of MreB and PBP2 overlaps with the maturation of the divisome as the late localizing proteins, including PBP3 and FtsN, start to accumulate at midcell approximately 20% of the division cycle later than FtsZ. Thus at about 40% of the division cycle time elongasomes and divisome proteins are simultaneously present at midcell (Fig. 3). In addition, the glycosyltransferase MurG responsible for the catalyses of Lipid I in Lipid II is present at midcell during the entire cell division process. In conclusion, key components for peptidoglycan synthesizes are present at midcell before constriction becomes visible.

The diameter remained constant at midcell between 0% and 40% of the division cycle. After 40% of the division cycle the midcell diameter started to decrease. This decline was unnoticeable by visual inspection. The cell diameter decreased clearly after 60% of the division cycle, which corresponds to the synthesis of the new cell poles (Figs 3 and 4). The period during which the elongasome proteins are present at midcell corresponds to the period in which the diameter decreases slowly and therefore this could be the phase of preseptal peptidoglycan synthesis. Preseptal peptidoglycan synthesis does not require any of the late localizing proteins (Varma *et al*., 2007; Varma and Young, 2009; Olrichs *et al*., 2011).

In addition, an interaction between PBP2 and the divisome proteins FtsQ, FtsW, PBP3 and FtsN was measured by FRET. FtsW and PBP3 from a precomplex (Fraipont *et al*., 2011). FtsN directly interacts with the early midcell localizing protein FtsA (Busiek *et al*., 2012) and from our timed localization is present at midcell together with PBP2. Therefore, it is not entirely surprising that these proteins interact with PBP2. Interestingly, we also see an interaction with FtsQ. This protein of which the function is unknown was found to interact with many divisome proteins by bacterial two-hybrid analyses and was therefore suggested to be the centre of the division machinery (Di Lallo *et al*., 2003). The most intriguing combination PBP2 and PBP3 was therefore investigated in more detail. Although the FRET efficiencies of the PBP2–PBP3 interaction were low, the results were reproducible and consistently and significantly higher than the background control that shows no interaction between PBP1A and PBP3. Additionally, no interaction between PBP2 and the PBP3 mutants could be measured by FRET. The mutants are incorporated efficiently in the cytoplasmic membrane but both lacked specific midcell localization. If the residue F24 would be essential for the interaction with PBP2, we would also find a loss of the FRET signal. Therefore, we cannot exclude that the loss of interaction between the PBP3 mutants and PBP2 is due to a decreased affinity for each other instead of an absence of interaction when PBP3 is not localizing at midcell.

However given the chance that one amino acid is essential for the interaction, we think that the more likely explanation is that the interaction between PBP2 and PBP3 occurs only at midcell. Interestingly, PBP2 and PBP3 are both required for cell division in chlamydia, an intracellular bacterium that lacks detectable amounts of peptidoglycan but whose cell division can be blocked with β-lactams (Ouellette *et al.,* 2012).

The rate of energy transfer between single donor and acceptor molecules is proportional to $1/r^6$, where r is the distance between the fluorophores. A fluorophore beta-barrel has a diameter of roughly 2.4 nm thus the fluorophores of mCherry and mKO are separated by at least 2.4 nm, which would yield 99% FRET efficiency (R_0 mKO–mCherry is 6.34 nm). At a distance of 12 nm between the fluorophores, the FRET efficiency has decreased to 2.1%. The E_{fA} gives the apparent FRET efficiency of the acceptor, where fA is the fraction of acceptors that participate in the energy transfer. As we do not know what the actual fraction of acceptor is that participate in the sensitized emission spectrum, we cannot calculate the absolute FRET efficiency. For the PBP2–PBP2 interaction the probability of mCherry–mKO formation is 50% as mCherry–mCherry and mKO–mKO combinations are also possible. In addition combinations between endogenous PBP2 and FP versions are expected as well. Therefore in reality the FRET efficiency is probably more than twice the level that is measured. Consequently, a large part of the PBP2 population probably occurs as a dimer in the cell. The FRET signal between PBP2 and PBP3 is diluted by the endogenous protein of which the exact concentration is not well established (Paradis-Bleau *et al*., 2010). In addition only the proteins that are present at midcell during a time window of 20% participate in the FRET signal. As the number of PBP2 and PBP3 proteins that colocalize at midcell is only a fraction of the total number of PBP2 and PBP3 molecules their physical proximity could be very close even with an E_{fA} of approximately 5% for their interaction. PBP2 and PBP3 could form heterodimers or interact with each other as two homodimers. Examples of proteins that form homodimers as well as heterodimers can be found in bacteria, for instance RscA and RscB of the Rcs phosphorelay (Majdalani and Gottesman, 2005). Alternatively, it is possible that other proteins mediate the interaction between PBP2 and PBP3.

The loss of catalytic activity of either PBP2 or PBP3 does not prevent their midcell localization (Fig. S7) or their

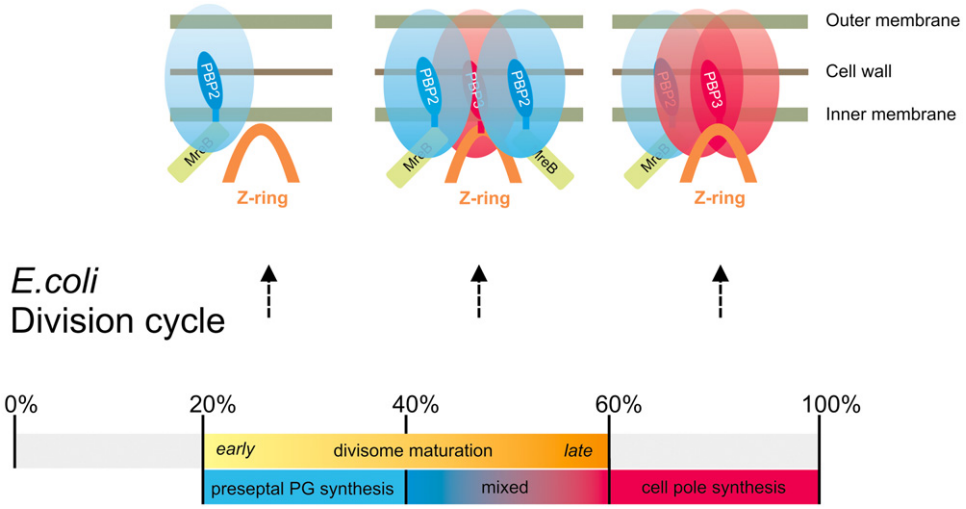

Fig. 6. Model of midcell localization of PBP2 and PBP3 during cell division for cells that are grown with a mass doubling of 85 min. After 20% of the division cycle time FtsZ proteins start to accumulate at midcell. The Z-ring structure will be formed and stabilized to initiate divisome maturation. Simultaneously some elongasome complexes (including at least MurG, MreB and PBP2) move to midcell and synthesize preseptal peptidoglycan. After about 40% of the division cycle the late proteins of the divisome complex begin to increase in concentration at midcell. More PBP3 proteins arrive and compete with PBP2 for peptidoglycan substrate. A mixed situation, in which elongasome and divisome PG synthases are both active, results in the slow decrease in midcell diameter of the cells between 40% and 60% of the division cycle. At 60% of the division cycle the divisome is mature and new cell pole synthesis occurs at a much faster rate. PBP2 is not present in the new cell poles and presumably does not contribute the new cell pole synthesis, although the presence of a minor amount of PBP2 at the leading edge of constriction cannot be excluded.

interaction as measure by FRET (data not shown). This suggests that their presence at midcell is dependent on other proteins such as MreB, MreC, MreD and RodA for PBP2 (Vats and Rothfield, 2007; Vats *et al*., 2009) and FtsZ and FtsW for PBP3 (Weiss *et al*., 1999; Mercer and Weiss, 2002; Fraipont *et al*., 2011). We propose that the formation of the Z-ring creates a barrier and positions the elongasome recruited by the MreB filaments at the constriction site and causes synthesis of a band of new peptidoglycan. It has been published that a GFP–MreB ring can be seen on both sides adjacent to the Z-ring (Vats and Rothfield, 2007). Unfortunately, the resolution of a wide field fluorescence microscope is not sufficient to determine whether this is the case in our immunolabelling experiments. Positioning of elongasomes on both sides of the Z-ring would be in accordance with published models, were the absence of MreB polymers are a prerequisite for septation (Vats and Rothfield, 2007; Jiang *et al*., 2011; Swulius and Jensen, 2012). Consequently, instead of a dispersed lipid II insertion the elongasomes continue to insert new material at midcell while PBP3 and the other, later localizing divisome proteins arrive and start to compete for the peptidoglycan building blocks available for cross-linking into the peptidoglycan layer. While the divisome matures and the number of PBP3 molecules increases, the elongasome is more and more excluded from the divisome until it does not participate anymore in midcell peptidoglycan synthesis. From this point onwards at about 60% of the division cycle rapid new cell pole synthesis is accomplished (Fig. 6). The cell may benefit from a slow start into cell pole synthesis in several ways: (i) the midcell position may be defined with good precision, (ii) the cell division site becomes defined at the site of cell wall synthesis preventing the simultaneous synthesis of more than one cell pole, and (iii) the elongasome may position the Mur enzymes for lipid II synthesis at the future division site to be used later by the divisome. The Mur enzymes have been shown to form a complex in association with the elongasome and divisome (Mohammadi *et al*., 2007; White *et al*., 2010) and they are the only enzymes that are shared by both synthetic protein machines. Finally, the growth and elongation of bacteria occurs exponentially. Because cell poles contribute to cell length the cell elongation at the side-wall has to slow down during cell division (Wientjes and Nanninga, 1989). A competition between elongasome and divisome proteins at midcell would slow down length growth sufficiently to maintain an overall exponential growth.

In conclusion, we have provided evidence for the colocalization of and interaction between PBP2 and PBP3 at midcell during a preparative phase in cell division that possibly coincides with preseptal peptidoglycan synthesis (Fig. 6). What the exact purpose is for this interaction remains to be elucidated as well as which of the elongasome proteins is the driving force for the association with the FtsZ ring.

Experimental procedures

Bacterial strains and growth conditions

All *E. coil* strains and the plasmids used in this work are listed in Table S1. For immunolabelling of wild-type cells for the division cycle timing of the localization of proteins, cells were grown to steady state in glucose minimal medium (GB1) containing 6.33 g of $K_2HPO_4{\cdot}3H_2O$, 2.95 g of KH_2PO_4, 1.05 g of $(NH_4)_2SO_4$, 0.10 g of $MgSO_4{\cdot}7H_2O$, 0.28 mg of $FeSO_4{\cdot}7H_2O$, 7.1 mg of $Ca(NO_3)_2{\cdot}4H_2O$, 4 mg of thiamine, 4 g of glucose and 50 mg of required amino acids, per litre pH 7.0 at 28°C as described (den Blaauwen *et al*., 1999). For all other immunolabelling experiments cells were grown in GB1 or in TY (10 g of trypton, 5 g of yeast extract, 5 g of NaCl per litre, pH 7.0) as specified. Absorbance was measured at 450 nm (GB1) or 600 (TY) with a Biochrom Libra S70. The generation times of the LMC500 strain grown in TY and GB1 medium are 40 and 85 min respectively.

Construction of the plasmids

Plasmids pWA003 and pWA004 were constructed by digesting pSAV047 and pSAV058 (Alexeeva *et al*., 2010) with EcoRI and HindIII, the *mrdA* gene was subsequently introduced by ligating after it was cut from pTB017 (den Blaauwen *et al*., 2003) using identical restriction enzymes. The mutant *ftsI* genes F24A and IFI were multiplied by PCR from plasmids pDSW643 and pDSW249 (Weiss *et al*., 1999) using the primers listed in Table S2. After restricting both PCR products and the pSAV047 plasmid with EcoRI and HindIII the fragments were ligated to produce vectors pRP004 and pRP005. The mKO–PBP1A 'gamma' fusion protein was expressed from the pBB004 plasmid. The plasmid was constructed in two steps; first a PCR was performed to produce copies of the 5′ end of the *mrcA* gene. The PCR product was cut with EcoRI and XhoI and ligated in the corresponding sites of pWA001. Subsequently, the complete *mrcA* was (as annotated EG10748) transferred to pSA069 using restriction sites EcoRI and HindIII. In this was the *ftsW* is removed from pSA069 and is replaced with *mrcA* (Fraipont *et al*., 2011).

Immunolocalization experiments

Escherichia coli cells fixed while shaking in growth medium as described (den Blaauwen *et al*., 2003). Cells were permeabilized and immunolabelled with antibodies as described by den Blaauwen *et al*. (2003). Cy3-conjugated Fab against MreB was purified against the MreB operon deletion strain PA340-678 (Wachi *et al*., 1987), against MurG (Mohammadi *et al*., 2007), PBP2 and PBP3 were affinity purified against purified protein (as described for PBP3; Bertsche *et al*., 2006) The affinity-purified serum against PBP3 was further purified against LMC510 cells grown for two mass doublings at 42°C. Antisera against FtsZ and FtsN were specific without further purification. Examples showing the reproducibility of the immunolabelling method are shown in Fig. S3A and B. Figure 3C and D shows that the immunolabelling procedure does not change the localization of membrane proteins.

Microscopy and image analysis

For immunolocalization imaging the cells were immobilized on 1% agarose (Koppelman *et al*., 2004), and photographed with a CoolSnap *fx* (Photometrics) CCD camera mounted on an Olympus BX-60 fluorescence microscope through a UPLANFI 100×/1.3 oil objective (Japan). Images were acquired with Micro-Manager (http://www.micro-manager.org/) with direct output of the desired hyperstack structure for ImageJ by Wayne Rasband (http://imagej.nih.gov/ij/). In all experiments the cells were first photographed in phase-contrast mode, then with the Cy3 filter (U-MNG, ex. 530–550 nm). In the first channel (phase contrast), the length and diameter of the cells were determined; the second channel was used to analyse the fluorescence signal. Image analysis was performed with the public domain program Coli-Inspector running under plugin ObjectJ written by Norbert Vischer (University of Amsterdam, http://simon.bio.uva.nl/objectj/), which runs in combination with ImageJ. From a map that shows the fluorescence profiles of each individual cell sorted to length [similar to demographs (Hocking *et al*., 2012)] the average fluorescence profile of all cells is plotted against the normalized length of the cells as described (Potluri *et al*., 2010). Fluorescence Centre Plus displays additional photons found in the cell centre. It is calculated from: FCplus = (centreConc – offCentreConc) * centreVol. Here the 'offCentre concentration' is regarded as 'cell background', and the total amount of extra photons in the cell centre (midcell ± 0.4 μm) is calculated. The value can be negative if the centre has less intensity than the peripheral parts of the cell. Age is expressed relative (0 to 100%), and is derived from the cell length ('Axis'). The cell lengths are sorted, and to calculate the age of an individual cell, the rank of its length is converted into a fractional value of 0 to 100%, assuming a logarithmic growth of the cell length (Aarsman *et al*., 2005). Indicating relative age does not require knowledge about the doubling time.

FRET experiment

For the FRET experiment we use a red-shifted fluorescent protein pair with mKO (Karasawa *et al*., 2004) as a donor and mCherry (Shaner *et al*., 2004) as an acceptor. *E. coli* LMC500 was co-transformed with two appropriate vectors. When a single protein was to be expressed a none-coding second plasmid was co-transformed. Each experiment included the mKO–mCherry tandem fusion as a positive control, mKO and mCherry expressed as two separate proteins in the cell, mCherry–PBP3 expressed with mKO–PBP1A as negative control. Transformants were grown and prepared for FRET measurements as described (Alexeeva *et al*., 2010). FRET efficiency was measured as described (Alexeeva *et al*., 2010) apart from the use of different filters. The following filters were used to obtain mCherry spectra: excitation filter 587/25 nm in combination with a 600-long pass emission filter and for mKO spectra a 541/12 nm excitation filter with a 550-long pass filter. For each experiment reference spectra were recorded from cells expressing only mKO, only mCherry proteins, and reference background spectra were recorded from cells bearing two none-coding plasmids. The reference spectra were used to calculate contributions of donor, acceptor and background to the total spectrum of the experimental

samples measured at λ_D using least square fitting. Sensitized emission and apparent efficiency of energy transfer E_{fA} were derived as described (Clegg, 1992; Clegg *et al*., 1992; Gadella, 2008; Alexeeva *et al*., 2010).

Data analysis

The FRET efficiency values have been estimated by the method of spectral unmixing as described in Alexeeva *et al*. (2010). From a set of multiple experiments a consensus mean and standard error of the mean was calculated for each construct using the Mandel–Paule algorithm (Paule and Mandel, 1982). The standard errors of the estimated FRET efficiency values that were obtained from the fit were used as weighting factors. In order to account for small sample sizes, the coverage factor used to calculate the 95% confidence intervals were based on the Student's *t*-distribution. Two-tailed and one-tailed Welch *t*-tests (Welch, 1947) with unequal variances and unequal sample size (the effective degrees of freedom was approximated using the Welch–Satterthwaite equation) were performed to test differences between the mean values of different constructs for statistical significance and to test whether mean values were higher than zero FRET. The complete statistical analysis was implemented in Matlab. All the statistical results can be found in the supporting information file for the interactions between PBP2–PBP3 and PBP2–divisome proteins, Tables S3, S4 and supplementary data respectively.

Acknowledgements

R.v.d.P., J.V., N.O.E.V., T.d.B. and W.V. were supported by the DIVINOCELL project of the European Commission (FP7-Health-2007-B-223431). T.d.B. and S.A. were supported by the Dutch NWO 'Van Molecuul tot Cel' programme grant (ALW 805.47.200). M.P. was supported by the Dutch NWO 'VIDI' grant (ALW 864.09.015). We thank David Weiss for the gift of PBP3 plasmids and Bart van den Berg van Saparoea for the pBB004 plasmid.

References

Aaron, M., Charbon, G., Lam, H., Schwarz, H., Vollmer, W., and Jacobs-Wagner, C. (2007) The tubulin homologue FtsZ contributes to cell elongation by guiding cell wall precursor synthesis in *Caulobacter crescentus*. *Mol Microbiol* **64:** 938–952.

Aarsman, M.E., Piette, A., Fraipont, C., Vinkenvleugel, T.M., Nguyen-Disteche, M., and den Blaauwen, T. (2005) Maturation of the *Escherichia coli* divisome occurs in two steps. *Mol Microbiol* **55:** 1631–1645.

Alexeeva, S., Gadella, T.W., Jr, Verheul, J., Verhoeven, G.S., and den Blaauwen, T. (2010) Direct interactions of early and late assembling division proteins in *Escherichia coli* cells resolved by FRET. *Mol Microbiol* **77:** 384–398.

Banzhaf, M., van den Berg van Saparoea, B., Terrak, M., Fraipont, C., Egan, A., Philippe, J., *et al*. (2012) Cooperativity of peptidoglycan synthases active in bacterial cell elongation. *Mol Microbiol* **85:** 179–194.

Bendezu, F.O., Hale, C.A., Bernhardt, T.G., and de Boer, P.A. (2009) RodZ (YfgA) is required for proper assembly of the MreB actin cytoskeleton and cell shape in *E. coli*. *EMBO J* **28:** 193–204.

Bertsche, U., Kast, T., Wolf, B., Fraipont, C., Aarsman, M.E., Kannenberg, K., *et al*. (2006) Interaction between two murein (peptidoglycan) synthases, PBP3 and PBP1B, in *Escherichia coli*. *Mol Microbiol* **61:** 675–690.

Bi, E.F., and Lutkenhaus, J. (1991) FtsZ ring structure associated with division in *Escherichia coli*. *Nature* **354:** 161–164.

den Blaauwen, T., Buddelmeijer, N., Aarsman, M.E., Hameete, C.M., and Nanninga, N. (1999) Timing of FtsZ assembly in *Escherichia coli*. *J Bacteriol* **181:** 5167–5175.

den Blaauwen, T., Aarsman, M.E., Vischer, N.O., and Nanninga, N. (2003) Penicillin-binding protein PBP2 of *Escherichia coli* localizes preferentially in the lateral wall and at mid-cell in comparison with the old cell pole. *Mol Microbiol* **47:** 539–547.

den Blaauwen, T., de Pedro, M.A., Nguyen-Disteche, M., and Ayala, J.A. (2008) Morphogenesis of rod-shaped sacculi. *FEMS Microbiol Rev* **32:** 321–344.

Busiek, K.K., Eraso, J.M., Wang, Y., and Margolin, W. (2012) The early divisome protein FtsA interacts directly through its 1c subdomain with the cytoplasmic domain of the late divisome protein FtsN. *J Bacteriol* **194:** 1989–2000.

Clegg, R.M. (1992) Fluorescence resonance energy transfer and nucleic acids. *Methods Enzymol* **211:** 353–388.

Clegg, R.M., Murchie, A.I., Zechel, A., Carlberg, C., Diekmann, S., and Lilley, D.M. (1992) Fluorescence resonance energy transfer analysis of the structure of the four-way DNA junction. *Biochemistry* **31:** 4846–4856.

Di Lallo, G., Fagioli, M., Barionovi, D., Ghelardini, P., and Paolozzi, L. (2003) Use of a two-hybrid assay to study the assembly of a complex multicomponent protein machinery: bacterial septosome differentiation. *Microbiology* **149:** 3353–3359.

Dominguez-Escobar, J., Chastanet, A., Crevenna, A.H., Fromion, V., Wedlich-Soldner, R., and Carballido-Lopez, R. (2011) Processive movement of MreB-associated cell wall biosynthetic complexes in bacteria. *Science* **333:** 225–228.

Dougherty, T.J., Kennedy, K., Kessler, R.E., and Pucci, M.J. (1996) Direct quantitation of the number of individual penicillin-binding proteins per cell in *Escherichia coli*. *J Bacteriol* **178:** 6110–6115.

Fraipont, C., Alexeeva, S., Wolf, B., van der Ploeg, R., Schloesser, M., den Blaauwen, T., and Nguyen-Disteche, M. (2011) The integral membrane FtsW protein and peptidoglycan synthase PBP3 form a subcomplex in *Escherichia coli*. *Microbiology* **157:** 251–259.

Fu, G., Huang, T., Buss, J., Coltharp, C., Hensel, Z., and Xiao, J. (2010) *In vivo* structure of the *E. coli* FtsZ-ring revealed by photoactivated localization microscopy (PALM). *PLoS ONE* **5:** e12682.

Gadella, T.W.J. (ed.) (2008) *FRET and FLIM Techniques*. Pillai, S., and van der Vliet, P.C. (eds). Amsterdam: Elsevier Science & Technology.

Garner, E.C., Bernard, R., Wang, W., Zhuang, X., Rudner, D.Z., and Mitchison, T. (2011) Coupled, circumferential motions of the cell wall synthesis machinery and MreB filaments in *B. subtilis*. *Science* **333:** 222–225.

Goehring, N.W., and Beckwith, J. (2005) Diverse paths to

midcell: assembly of the bacterial cell division machinery. *Curr Biol* **15:** R514–R526.
Hale, C.A., and de Boer, P.A. (2002) ZipA is required for recruitment of FtsK, FtsQ, FtsL, and FtsN to the septal ring in *Escherichia coli*. *J Bacteriol* **184:** 2552–2556.
Hocking, J., Priyadarshini, R., Takacs, C.N., Costa, T., Dye, N.A., Shapiro, L., *et al*. (2012) Osmolality-dependent relocation of penicillin-binding protein PBP2 to the division site in *Caulobacter crescentus*. *J Bacteriol* **194:** 3116–3127.
Jiang, H., Si, F., Margolin, W., and Sun, S.X. (2011) Mechanical control of bacterial cell shape. *Biophys J* **101:** 327–335.
Jones, L.J., Carballido-Lopez, R., and Errington, J. (2001) Control of cell shape in bacteria: helical, actin-like filaments in *Bacillus subtilis*. *Cell* **104:** 913–922.
Karasawa, S., Araki, T., Nagai, T., Mizuno, H., and Miyawaki, A. (2004) Cyan-emitting and orange-emitting fluorescent proteins as a donor/acceptor pair for fluorescence resonance energy transfer. *Biochem J* **381:** 307–312.
Karczmarek, A., Martinez-Arteaga, R., Alexeeva, S., Hansen, F.G., Vicente, M., Nanninga, N., and den Blaauwen, T. (2007) DNA and origin region segregation are not affected by the transition from rod to sphere after inhibition of *Escherichia coli* MreB by A22. *Mol Microbiol* **65:** 51–63.
Koppelman, C.M., Aarsman, M.E., Postmus, J., Pas, E., Muijsers, A.O., Scheffers, D.J., *et al*. (2004) R174 of *Escherichia coli* FtsZ is involved in membrane interaction and protofilament bundling, and is essential for cell division. *Mol Microbiol* **51:** 645–657.
Kruse, T., Bork-Jensen, J., and Gerdes, K. (2005) The morphogenetic MreBCD proteins of *Escherichia coli* form an essential membrane-bound complex. *Mol Microbiol* **55:** 78–89.
Majdalani, N., and Gottesman, S. (2005) The rcs phosphorelay: a complex signal transduction system. *Annu Rev Microbiol* **59:** 379–405.
Mercer, K.L., and Weiss, D.S. (2002) The *Escherichia coli* cell division protein FtsW is required to recruit its cognate transpeptidase, FtsI (PBP3), to the division site. *J Bacteriol* **184:** 904–912.
Mohammadi, T., Karczmarek, A., Crouvoisier, M., Bouhss, A., Mengin-Lecreulx, D., and den Blaauwen, T. (2007) The essential peptidoglycan glycosyltransferase MurG forms a complex with proteins involved in lateral envelope growth as well as with proteins involved in cell division in *Escherichia coli*. *Mol Microbiol* **65:** 1106–1121.
Mohammadi, T., van Dam, V., Sijbrandi, R., Vernet, T., Zapun, A., Bouhss, A., *et al*. (2011) Identification of FtsW as a transporter of lipid-linked cell wall precursors across the membrane. *EMBO J* **30:** 1425–1432.
Olrichs, N.K., Aarsman, M.E., Verheul, J., Arnusch, C.J., Martin, N.I., Herve, M., *et al*. (2011) A novel *in vivo* cell-wall labeling approach sheds new light on peptidoglycan synthesis in *Escherichia coli*. *Chembiochem* **12:** 1124–1133.
Ouellette, S.P., Karimova, G., Subtil, A., and Ladant, D. (2012) PBP2 used for division in *Chlamydia*. *Mol Microbiol* **85:** 164–178.
Paradis-Bleau, C., Markovski, M., Uehara, T., Lupoli, T.J., Walker, S., Kahne, D.E., and Bernhardt, T.G. (2010) Lipoprotein cofactors located in the outer membrane activate bacterial cell wall polymerases. *Cell* **143:** 1110–1120.
Pastoret, S., Fraipont, C., den Blaauwen, T., Wolf, B., Aarsman, M.E., Piette, A., *et al*. (2004) Functional analysis of the cell division protein FtsW of *Escherichia coli*. *J Bacteriol* **186:** 8370–8379.
Paule, R., and Mandel, J. (1982) Consensus values and weighting factors. *J Res Natl Bur Stand* **87:** 377–385.
de Pedro, M.A., Quintela, J.C., Holtje, J.V., and Schwarz, H. (1997) Murein segregation in *Escherichia coli*. *J Bacteriol* **179:** 2823–2834.
Piette, A., Fraipont, C., den Blaauwen, T., Aarsman, M.E., Pastoret, S., and Nguyen-Disteche, M. (2004) Structural determinants required to target penicillin-binding protein 3 to the septum of *Escherichia coli*. *J Bacteriol* **186:** 6110–6117.
Potluri, L., Karczmarek, A., Verheul, J., Piette, A., Wilkin, J.M., Werth, N., *et al*. (2010) Septal and lateral wall localization of PBP5, the major d,d-carboxypeptidase of *Escherichia coli*, requires substrate recognition and membrane attachment. *Mol Microbiol* **77:** 300–323.
Potluri, L., Kannan, S., and Young, K.D. (2012) ZipA is required for FtsZ-dependent preseptal peptidoglycan synthesis prior to invagination during cell division. *J Bacteriol* **194:** 5334–5342.
Reshes, G., Vanounou, S., Fishov, I., and Feingold, M. (2008) Timing the start of division in *E. coli:* a single-cell study. *Phys Biol* **5:** 046001–046009.
Salje, J., van den Ent, F., de Boer, P., and Lowe, J. (2011) Direct membrane binding by bacterial actin MreB. *Mol Cell* **43:** 478–487.
Sauvage, E., Kerff, F., Terrak, M., Ayala, J.A., and Charlier, P. (2008) The penicillin-binding proteins: structure and role in peptidoglycan biosynthesis. *FEMS Microbiol Rev* **32:** 234–258.
Shaner, N.C., Campbell, R.E., Steinbach, P.A., Giepmans, B.N., Palmer, A.E., and Tsien, R.Y. (2004) Improved monomeric red, orange and yellow fluorescent proteins derived from discosoma sp. red fluorescent protein. *Nat Biotechnol* **22:** 1567–1572.
Spratt, B.G. (1975) Distinct penicillin binding proteins involved in the division, elongation, and shape of *Escherichia coli* K12. *Proc Natl Acad Sci USA* **72:** 2999–3003.
Swulius, M.T., and Jensen, G.J. (2012) The helical MreB cytoskeleton in *E. coli* MC1000/ pLE7 is an artifact of the N-terminal YFP tag. *J Bacteriol* **194:** 6382–6386 doi:10.1128/JB.00505-12.
van Teeffelen, S., Wang, S., Furchtgott, L., Huang, K.C., Wingreen, N.S., Shaevitz, J.W., and Gitai, Z. (2011) The bacterial actin MreB rotates, and rotation depends on cell-wall assembly. *Proc Natl Acad Sci USA* **108:** 15822–15827.
Typas, A., Banzhaf, M., van den Berg van Saparoea, B., Verheul, J., Biboy, J., Nichols, R.J., *et al*. (2010) Regulation of peptidoglycan synthesis by outer-membrane proteins. *Cell* **143:** 1097–1109.
Typas, A., Banzhaf, M., Gross, C.A., and Vollmer, W. (2011) From the regulation of peptidoglycan synthesis to bacterial growth and morphology. *Nat Rev Microbiol* **10:** 123–136.
Varma, A., and Young, K.D. (2009) In *Escherichia coli,* MreB and FtsZ direct the synthesis of lateral cell wall via independent pathways that require PBP 2. *J Bacteriol* **191:** 3526–3533.
Varma, A., de Pedro, M.A., and Young, K.D. (2007) FtsZ

directs a second mode of peptidoglycan synthesis in *Escherichia coli*. *J Bacteriol* **189:** 5692–5704.
Vats, P., and Rothfield, L. (2007) Duplication and segregation of the actin (MreB) cytoskeleton during the prokaryotic cell cycle. *Proc Natl Acad Sci USA* **104:** 17795–17800.
Vats, P., Shih, Y.L., and Rothfield, L. (2009) Assembly of the MreB-associated cytoskeletal ring of *Escherichia coli*. *Mol Microbiol* **72:** 170–182.
Vinella, D., Joseleau-Petit, D., Thévenet, D., Bouloc, P., and D'Ari, R. (1993) Penicillin-binding protein 2 inactivation in *Escherichia coli* results in cell division inhibition, which is relieved by FtsZ overexpression. *J Bacteriol* **175:** 6704–6710.
Vollmer, W., and Bertsche, U. (2008) Murein (peptidoglycan) structure, architecture and biosynthesis in *Escherichia coli*. *Biochim Biophys Acta* **1778:** 1714–1734.
Wachi, M., Doi, M., Tamaki, S., Park, W., Nakajima-Iijima, S., and Matsuhashi, M. (1987) Mutant isolation and molecular cloning of *mre* genes, which determine cell shape, sensitivity to mecillinam, and amount of penicillin-binding proteins in *Escherichia coli*. *J Bacteriol* **169:** 4935–4940.
Wang, S., Furchtgott, L., Huang, K.C., and Shaevitz, J.W. (2012) Helical insertion of peptidoglycan produces chiral ordering of the bacterial cell wall. *Proc Natl Acad Sci USA* **109:** E595–E604.
Wang, X., Huang, J., Mukherjee, A., Cao, C., and Lutkenhaus, J. (1997) Analysis of the interaction of FtsZ with itself, GTP, and FtsA. *J Bacteriol* **179:** 5551–5559.
Weiss, D.S., Chen, J.C., Ghigo, J.M., Boyd, D., and Beckwith, J. (1999) Localization of FtsI (PBP3) to the septal ring requires its membrane anchor, the Z ring, FtsA, FtsQ, and FtsL. *J Bacteriol* **181:** 508–520.
Welch, B.L. (1947) The generalisation of student's problems when several different population variances are involved. *Biometrika* **34:** 28–35.
White, C.L., Kitich, A., and Gober, J.W. (2010) Positioning cell wall synthetic complexes by the bacterial morphogenetic proteins MreB and MreD. *Mol Microbiol* **76:** 616–633.
Wientjes, F.B., and Nanninga, N. (1989) Rate and topography of peptidoglycan synthesis during cell division in *Escherichia coli:* concept of a leading edge. *J Bacteriol* **171:** 3412–3419.
Wissel, M.C., Wendt, J.L., Mitchell, C.J., and Weiss, D.S. (2005) The transmembrane helix of the *Escherichia coli* division protein FtsI localizes to the septal ring. *J Bacteriol* **187:** 320–328.

Supporting information

Additional supporting information may be found in the online version of this article.